fermentation

MDPI

Article

The Potential of Arctic *Pseudogymnoascus* Fungi in the Biosynthesis of Natural Products

Tatiana V. Antipova [1,*], Kirill V. Zaitsev [2,*], Valentina P. Zhelifonova [1], Sergey V. Tarlachkov [1], Yuri K. Grishin [2], Galina A. Kochkina [1] and Mikhail B. Vainshtein [1]

[1] G.K. Skryabin Institute of Biochemistry and Physiology of Microorganisms, FRC Pushchino Scientific Centre of Biological Research, Russian Academy of Sciences, 142290 Pushchino, Russia; zhelifonova@yandex.ru (V.P.Z.); sergey@tarlachkov.ru (S.V.T.); gaga56@mail.ru (G.A.K.); vain@ibpm.pushchino.ru (M.B.V.)

[2] Department of Chemistry, M.V. Lomonosov Moscow State University, 119991 Moscow, Russia; grishin@nmr.chem.msu.ru

* Correspondence: tatantip@rambler.ru (T.V.A.); zaitsev@org.chem.msu.ru (K.V.Z.)

Abstract: Scarce research into the secondary metabolites of the fungi *Pseudogymnoascus* spp. has shown a hidden biosynthetic potential for biologically active compounds. This work investigated the biosynthesis of secondary metabolites by two *Pseudogymnoascus* fungal strains, VKM F-4518 and VKM F-4519, isolated from the surface soil layer of the Kolyma Lowland, Russia, in the Arctic. In these strains, 16-membered trilactone macrolides, (+)-macrosphelides A and B, were identified using 1D and 2D NMR, UHRMS, and optical rotation data. In the fungi of this genus, these metabolites were found for the first time. The studied strains are highly active producers of macrosphelide A, which is being considered as a promising agent for the cure of cancer. Using the antiSMASH secondary metabolite analysis tool, we found that the genome of strain VKM F-4518 contained 32 of the biosynthetic clusters of the secondary metabolite genes (BGC) and that of VKM F-4519 had 17 BGCs. Based on the comparison of the cluster of macrotriolide genes from the fungus *Paraphaeosphaeria sporulosa*, we found the complete supposed cluster BGCs of macrosphelides in the genomes of two *Pseudogymnoascus* strains using the BLAST+ program.

Keywords: fungi; secondary metabolites; natural compounds; biotechnology; macrolides; macrosphelides A and B; the Arctic; NMR spectroscopy; gene cluster

check for updates

Citation: Antipova, T.V.; Zaitsev, K.V.; Zhelifonova, V.P.; Tarlachkov, S.V.; Grishin, Y.K.; Kochkina, G.A.; Vainshtein, M.B. The Potential of Arctic *Pseudogymnoascus* Fungi in the Biosynthesis of Natural Products. *Fermentation* **2023**, *9*, 702. https://doi.org/10.3390/fermentation9080702

Academic Editor: Alexander A. Zhgun

Received: 21 June 2023
Revised: 21 July 2023
Accepted: 24 July 2023
Published: 26 July 2023

Copyright: © 2023 by the authors. Licensee MDPI, Basel, Switzerland. This article is an open access article distributed under the terms and conditions of the Creative Commons Attribution (CC BY) license (https://creativecommons.org/licenses/by/4.0/).

1. Introduction

Secondary metabolites (SM) are a promising object of research due to the possibility of discovering substances with a new mechanism of medical action and less toxicity. In this regard, the search for biologically active natural compounds is constantly ongoing in order to discover new and/or more effective drugs [1]. Fungi are well known as sources of diverse biologically active compounds [2,3]. Fungal SMs exhibit a variety of biological activities: they are used as antibiotics, fungicides, immunomodulators, antioxidants, and natural colorants [4–7]. For this reason, fungi are the most interesting object of special and close attention for searching for new biologically active compounds. The role of these microorganisms as the main drug sources for the pharmaceutical industry is known and obvious.

The variety of SMs identified in fungi is significant, and it is assumed that only a minority of all naturally occurring SMs are currently known [8]. The best-known SMs belong to four basic chemical families: polyketides, terpenoids, nonribosomal peptides, and a hybrid of nonribosomal peptides and polyketides [4]. As a rule, SMs are synthesized using primary metabolic substrates, among which, acetyl-CoA stands out as a precursor of polyketides and terpenoids [9]. Each SM biosynthetic pathway begins with a characteristic enzyme type and ends with the activity of other specific enzymes, which introduce

additional modifications to molecules. At present, more than 1000 fungal genomes are known and available as a result of achievements in proteomics, genomics, and sequencing methods [8]. Nevertheless, despite several decades of efforts towards discovering new compounds from fungi, the analysis of genomes for the presence of clusters of their biosynthetic genes is still quite limited [10].

The fungi *Pseudogymnoascus* spp. Railo 1929 with *Geomyces* anamorphs are widespread in nature and can be found almost everywhere, from the Arctic to the Antarctic [11–14]. They can exist in the marine environment and be spread by deep-sea currents [15]. Very often, they are isolated from low-temperature ecotopes. These fungi are not truly psychrophiles or halophiles, but are capable of developing in cold environments (even at slightly negative temperatures) with a reduced level of nutrition and increased salt content [16]. These conditions cause not only osmotic, but also oxidative stress. It is, therefore, natural that these fungi are capable of growth in microaerophilic conditions that reduce their consequences [17]. They are capable of changing their metabolism in response to complex abiotic conditions. In particular, they, rather than basidial fungi, were discovered in studies of the degradation of wood in a hut built by the Scott and Shackleton expeditions in 1908 at Cape Royds in Antarctica [18]. It has been proven that *Pseudogymnoascus* spp. have the ability to produce cold-adapted enzymes to survive in low-temperature habitats [19–23]. In particular, the fungus *Pseudogynmoascus pannorum* is capable of producing a protease, characterized by a high catalytic efficiency at low temperatures [22,24], which can play a significant role in the ability of this organism to survive in extreme conditions.

The fungi of the genus *Pseudogymnoascus* can be antagonists of potato scab pathogens in the soils of potato fields [19]. They are noted as some of the predominant microbial colonizers of the root endosphere and rhizosphere of turfgrass systems [23]. There are animal pathogens among the representatives of this genus. For instance, *Pseudogymnoascus destructans* causes white-nose syndrome in bats [24].

There are several studies on the secondary metabolites of the genus *Pseudogymnoascus* representatives. Most of the established structures belong to polyketides that exhibit antimicrobial activity [25–28]. Polyketides, asterric acid derivatives, and geomycins A–C have been isolated from *Geomyces* sp. (obtained from Antarctic soil) and have shown both antifungal and antibacterial activity [29]. *Geomyces pannorum*, isolated from leaf litter, produces pannomycin, a *cis*-decalin secondary metabolite with potential antibacterial activity against *Staphylococcus aureus* [30]. A *Pseudogymnoascus* strain isolated from marine sediments in Admiralty Bay (Antarctica) has suppressed the growth of the phytopathogenic bacteria *Xanthomonas passiflorae* and *Xanthomonas euvesicatoria* (99% and 98%, respectively) [31]. Red pigment amphiol, which has antifungal activity, has been isolated from strain *Pseudogymnoascus* sp. PF-1464 [25]. Mycocidal activity, in relation to *Cladosporium sphaerospermum*, similar to the activity of the drug benomyl, has been found in strain *Pseudogymnoascus* sp. from Antarctic sediments [32]. Research into the antimicrobial, cytotoxic, and antiprotozoal properties of the metabolites of Antarctic fungal communities isolated from the marine and lake sediments of Deception Island included a representative of the genus *Pseudogymnoascus* and had high selective activity against the fungus *Paracoccidioides brasiliensis* [33], which is one of the most hazardous fungal pathogens for humans. Six new tremulane sesquiterpenoids with antitumor activities have been found in Antarctic *Pseudogymnoascus* fungi [34]. On the whole, the scarce research into the secondary metabolites of *Pseudogymnoascus* fungi from cold environments has shown a hidden biosynthetic potential for the search for biologically active compounds.

In the present work, we investigated the secondary metabolites of the *Pseudogymnoascus* sp. strains, VKM F-4518 and VKM F-4519, isolated from the surface layer of sediments in the Kolyma Lowland (the Arctic). We report on the isolation and structure of two compounds, which have been identified as macrolide antibiotics macrosphelides A and B. Given the potential interest of these compounds, a suspected biosynthetic cluster of macrosphelides genes has been found.

2. Materials and Methods

Fungal strains. The strains of Pseudogymnoascus sp., VKM F-4518 and VKM F-4519, were isolated from the surface layer of sediments in the Kolyma Lowland in the Arctic. The complete genome of these strains was investigated earlier [14] and deposited in the GenBank under the numbers JPKC00000000.1 for *Pseudogymnoascus* sp. VKM F-4518 and JPKD00000000.1 for *Pseudogymnoascus* sp. VKM F-4519. The strains are stored in the All-Russian Collection of Microorganisms (VKM), G.K. Skryabin Institute of Biochemistry and Physiology of Microorganisms, FRC Pushchino Scientific Centre of Biological Research, Russian Academy of Sciences.

Growth conditions. The strains of Pseudogymnoascus sp. were grown on malt agar slants for 7 days. Then, an aqueous spore suspension (1–2 $\times$ 10^5 conidia/mL) of each strain was inoculated into 3 $\times$ 750 mL Erlenmeyer flasks, each containing 150 mL of medium (g/L of distilled water): mannitol—50.0; succinic acid—5.4; $MgSO_4 \times 7H_2O$—0.3; and KH_2PO_4—1.0; with a pH adjusted to 5.4 with 25% NH_4OH solution for submerged cultivation on a shaker (220 rpm) at 24 $\pm$ 1 °C. The sampling was conducted in 11 days.

Isolation and identification of the metabolites. The grown mycelium was separated from the culture liquid by filtration through a cotton filter. The filtrate was acidified with a 3% solution of tartaric acid to pH 4 and extracted with $CHCl_3$ (*v*/*v*) three times at room temperature. Then, all the volatile materials were removed in vacuo. The amounts of the studied extracts of strain *Pseudogymnoascus* sp. VKM F-4518 and strain *Pseudogymnoascus* sp. VKM F-4519 obtained were, respectively, 267 mg and 166 mg.

The extracts of the culture liquid were analyzed using TLC on silica gel plates in chloroform–methanol–25% NH_4OH (90:10:0.1) (eluent I) and chloroform–acetone (93:7) (eluent II) systems. The metabolites were detected using absorption and fluorescence at 254 and 366 nm. An extract of strain VKM F-4518 was used to isolate the metabolites using column chromatography, since it contained a larger amount of target products. The extract was loaded onto a column (3 $\times$ 11 cm) filled with silica gel (Silica gel 60, 0.063–0.1 mm, Merck, Germany). Elution was carried out in a gradient of $CHCl_3$ and $CHCl_3$:MeOH (9:1) to yield six fractions (Fr. 1–Fr. 6). Fr. 4 yielded macrosphelide **1** (125 mg). The final purification of compound **2** was achieved using preparative TLC on a silica gel plates of Fr. 2 using eluent II (50 mg).

^{1}H NMR (400.130 MHz) and ^{13}C NMR (100.613 MHz) spectra were recorded with an Agilent 400MR spectrometer at 298 K. Chemical shifts are given in ppm relative to internal Me_4Si. The methanol was purified using reflux and distillation over Mg turnings. Optical rotations were measured with a JASCO DIP-1000 digital polarimeter at ambient temperature using a 100 nm cell with a 2 mL capacity. High-resolution mass spectra (UHRMS) were acquired using a commercial 7 Tesla LTQ FT ultra mass spectrometer equipped with an Ion Max electrospray ion source (Thermo Electron Corp., Bremen, Germany). Chemical ionization mass spectra (CI) were registered on an LCQ Advantage MAX quadrupole mass spectrometer (Thermo Fisher Scientific GmbH, Bremen, Germany), using a single-channel syringe pump for the direct injection of a specimen into the chamber for chemical ionization at atmospheric pressure. Column chromatography was performed on silica gel (Silica gel 60, 0.063–0.1 mm, Merck, Germany). Silica gel plates (Silica gel F_{254}, Merck, Germany) were used for thin-layer chromatography (TLC) assays.

Bioinformatic analysis. The search for the macrosphelide biosynthesis genes was carried out in the genomes of *Pseudogymnoascus* sp. VKM F-4518 (JPKC00000000.1) and Pseudogymnoascus sp. VKM F-4519 (JPKD00000000.1) using the BLAST+ program [35]. The protein sequences of the macrosphelide biosynthesis genes from strain *Paraphaeosphaeria sporulosa* AP3s5-JAC2a [36] were used as references. The identities between the protein sequences were calculated using the TaxonDC program [37]. The antiSMASH program (fungal version) was used for a bioinformatic analysis of the biosynthetic clusters of the secondary metabolite genes (BCG) in the genomes of the strains.

Macrosphelide A (**1**). White powder.

^{1}H NMR (400 MHz, $CDCl_3$, RT): δ 6.84 (dd, $^{3}J_{H\text{-}H}$ 15.7, 9.5 Hz, 1H, H-7), 6.82 (dd, $^{3}J_{H\text{-}H}$ 15.6, 9.2 Hz, 1H, H-13), 5.98 (dd, $^{3}J_{H\text{-}H}$ 15.6, $^{4}J_{H\text{-}H}$ 1.4 Hz, 1H, H-12), 5.95 (dd, $^{3}J_{H\text{-}H}$ 15.7, $^{4}J_{H\text{-}H}$ 1.4 Hz, 1H, H-6), 5.35-5.25 (m, 1H, H-3), 4.94-4.85 (m, 1H, H-9), 4.84-4.76 (m, 1H, H-15), 4.16-4.12 (m, 1H, H-8), 4.08-4.03 (m, 1H, H-14), 3.94 (br s, 1H, OH), 3.80 (br s, 1H, OH), 2.56 (br s, 1H, H-2), 2.55 (br s, 1H, H-2), 1.38 (d, $^{3}J_{H\text{-}H}$ 6.5 Hz, 3H, Me-9), 1.31 (d, $^{3}J_{H\text{-}H}$ 6.5 Hz, 3H, Me-15), and 1.28 (d, $^{3}J_{H\text{-}H}$ 6.5 Hz, 3H, Me-3) ppm.

^{13}C NMR (400 MHz, $CDCl_3$, RT): δ 170.10 (C-1), 165.74 (C-11), 165.05 (C-5), 146.54 (C-13), 145.87 (C-7), 122.43 (C-6), 121.99 (C-12), 74.35 (C-9), 74.09 (C-8), 73.43 (C-15), 72.72 (C-14), 67.75 (C-3), 40.86 (C-2), 19.52 (Me-3), 17.75 (Me-9), and 17.60 (Me-15) ppm.

Macrosphelide B (**2**). Yellowish powder.

^{1}H NMR (400 MHz, $CDCl_3$, RT): δ 7.01 (d, $^{3}J_{H\text{-}H}$ 15.7 Hz, 1H, H-12), 6.90 (dd, $^{3}J_{H\text{-}H}$ 15.8, 3.8 Hz, 1H, H-7), 6.72 (d, $^{3}J_{H\text{-}H}$ 15.7 Hz, 1H, H-13), 6.07 (dd, $^{3}J_{H\text{-}H}$ 15.8, $^{4}J_{H\text{-}H}$ 2.0 Hz, 1H, H-6), 5.47-5.40 (m, 1H, H-3), 5.08-5.01 (m, 2H, H-9/H-15), 4.32-4.28 (m, 1H, H-8), 2.81 (dd, $^{2}J_{H\text{-}H}$ 16.2, $^{3}J_{H\text{-}H}$ 11.2 Hz, 1H, H-2), 2.61 (dd, $^{2}J_{H\text{-}H}$ 16.2, $^{3}J_{H\text{-}H}$ 2.3 Hz, 1H, H-2), 1.48 (d, $^{3}J_{H\text{-}H}$ 6.8 Hz, 3H, Me-9), 1.42 (d, $^{3}J_{H\text{-}H}$ 7.8 Hz, 3H, Me-15), 1.34 (d, $^{3}J_{H\text{-}H}$ 6.4 Hz, 3H, Me-3), and 1.23 (br s, 1H, OH) ppm.

^{13}C NMR (400 MHz, $CDCl_3$, RT): δ 196.19 (C-14), 170.33 (C-1), 165.30 (C-11), 164.23 (C-5), 144.37 (C-7), 132.54 (C-13), 132.05 (C-12), 122.50 (C-6), 76.71 (C-15), 75.75 (C-9), 74.73 (C-8), 67.70 (C-3), 40.59 (C-2), 19.77 (Me-3), 17.88 (Me-9), and 16.04 (Me-15) ppm.

3. Results

The extracts of the strains *Pseudogymnoascus* sp. VKM F-4518 and VKM F-4519 culture liquid contained metabolites **1** with R_f 0.41 (eluent I, see Experiment) and **2** with R_f 0.62 (eluent I). Compound **1** was obtained as a white powder, m.p. 146 °C, and compound **2** was isolated as a yellowish powder, m.p. 146–147 °C. The CI mass spectrum of **1** and **2** (positive ions) displayed molecular ions at m/z 343.0 $[M + H]^+$ and at m/z 340.8 $[M + H]^-$, respectively (see Supporting Information Figure S1). The exact molecular formulas of compounds **1** and **2** were determined using UHRMS operating in positive ion mode, giving $[M_1 + H]^+ = C_{16}H_{22}O_8$ (m/z = 343.13871) and $[M_2 + H]^+ = C_{16}H_{20}O_8$ (m/z = 341.12424), respectively.

In the ^{1}H NMR spectrum of **1** (Table S1, Figure S2), two sets of olefinic proton signals were observed at δ 5.95 (dd, $^{3}J_{H\text{-}H}$ 15.7, $^{4}J_{H\text{-}H}$ 1.4 Hz, 1H, H-6) and δ 6.84 (dd, $^{3}J_{H\text{-}H}$ 15.7, 9.5 Hz, 1H, H-7) ppm, and δ 5.98 (dd, $^{3}J_{H\text{-}H}$ 15.6, $^{4}J_{H\text{-}H}$ 1.4 Hz, 1H, H-12) and δ 6.82 (dd, $^{3}J_{H\text{-}H}$ 15.6, 9.2 Hz, 1H, H-13) ppm. These coupling constants ($^{3}J_{H\text{-}H}$ 15.6, 15.7 Hz) showed a *trans*-configuration of both CH=CH fragments. In the ^{13}C NMR spectrum of **1** (Table S1, Figures S3 and S4), 16 carbon signals were observed, which were assignable to three carbonyl (δ 165.05, 165.74, and 170.10 ppm); five methine (δ 67.75, 72.72, 73.43, 74.09, and 74.35 ppm); one methylene (δ 40.86 ppm); and three methyl (δ 17.60, 17.75, and 19.52 ppm) carbons. In this spectrum, these corresponding olefinic carbon signals were also observed at δ 122.43 (C-6), δ 145.87 (C-7), δ 121.99 (C-12), and δ 146.54 (C-13) ppm, respectively. In the ^{1}H-^{1}H COSY (Figure S5) and ^{1}H-^{13}C HSQC (Figure S6) and HMQC (Figure S7) spectra of **1**, the presence of partial structures (2→ 3 → 3Me), (6 → 7→ 8 → 9 → 9Me), and (12 → 13 → 14 → 15 → 15Me) of **1** was demonstrated (Figure 1). Finally, the structure of **1** was determined using HMBC (8 Hz) experiments, as shown in Figure 1.

Both **1** and **2** have similar NMR spectral characteristics (see Supporting Information; Tables S1 and S2, Figures S2–S14); the difference consists of significant signal shifts in the ^{13}C NMR spectra for atoms C12–15, due to the oxidation of hydroxyl C-14 in **1** to carbonyl at the transition to compound **2**. Another characteristic feature of **1** and **2** is the *E*-, *E*-configuration of both double bonds (the spin–spin coupling constants $^{3}J_{H\text{-}H}$ are 15.7–15.9 Hz). Interestingly, according to this and additional (for example, Nuclear Overhauser effect; Figure S9, Supporting Information) data, we may establish the relative configurations for metabolites **1** (*3S**, *8R**, *9S**, *14R**, and *15S**) and **2** (*3S**, *8R**, *9S**, and *15S**). Thus, for **1,** the cross-signals in the NOESY spectrum, δ 5.31/1.41, 4.90/1.30, and 4.15/1.31 ppm, may be identified as H3/Me-9, H9/Me-3, and H8/Me-15 interactions, respectively.

In general, based on the obtained results and the literature data, the NMR spectra for metabolites **1** and **2** (see Supporting Information) correspond to (+)-macrosphelide A and (+)-macrosphelide B, respectively (Figure 1) [38].

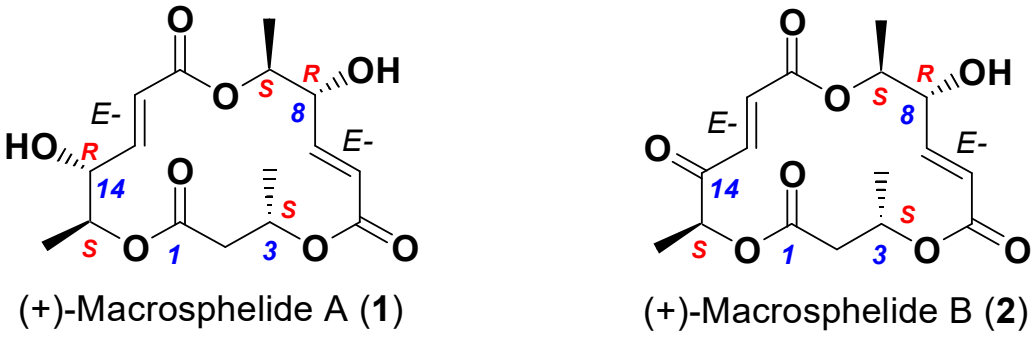

Figure 1. Structures of (+)-macrosphelides A and B.

As is evident, both compounds are chiral. For **1**, (+)-macrosphelide A, $[\alpha]^{24}_{D}$ +76.5 (c 0.031, MeOH) ($[\alpha]^{24}_{D}$ +84.1 (c 0.59, MeOH) [38]; $[\alpha]^{24}_{D}$ +82.0 (c 0.10, MeOH) [39]; $[\alpha]^{27}_{D}$ +82.0 (c 0.10, MeOH) [40]; $[\alpha]_{D}$ +74.3 (c 0.75, MeOH) [41]; $[\alpha]^{30}_{D}$ +85.0 (c 0.046, MeOH) [42]; and $[\alpha]^{25}_{D}$ +81.0 (c 0.195, MeOH) [43,44]. Its absolute configuration corresponds to (*3S*, *8R*, *9S*, *14R*, and *15S*). For **2**, (+)-macrosphelide B, $[\alpha]^{24}_{D}$ +3.8 (c 0.007, MeOH) ($[\alpha]^{20}_{D}$ +4.10 (c 0.99, MeOH) [38]; $[\alpha]^{24}_{D}$ +10.8 (c 0.065, MeOH) [45]; $[\alpha]^{24}_{D}$ +10.0 (c 0.39, MeOH) [40]; $[\alpha]^{26}_{D}$ +9.1 (c 0.154, MeOH) [42]; $[\alpha]^{20}_{D}$ +10.8 (c 0.065, MeOH) [46]; and $[\alpha]^{27}_{D}$ +3.71 (c 0.335, MeOH) [43,44]. Its absolute configuration is similar to **1**, i.e., it is (*3S*, *8R*, *9S*, and *15S*). The absolute configuration of (+)-macrosphelide A had been established earlier using XRD and chemical (Mosher esters) methods and was confirmed by the total synthesis [39]. Thus, the identity of metabolites **1** and **2** is unambiguously established using NMR spectroscopy, optic rotation, and UHRMS as (+)-macrosphelides A and B, respectively.

Earlier, Harvey et al. [36] reported that 41 fungal biosynthetic gene clusters from various fungal species had been heterologously expressed into Saccharomyces cerevisiae. This approach permits the detection of metabolites that are hardly detectable in the initial fungal organisms. The most notable is a cluster from the fungus *Paraphaeosphaeria sporulosa*, which contains genes of the enzymes hydrolase (SH), monooxygenases cytochrome P450 (p450), dehydratase (DH), short-chain dehydrogenase/reductase (SDR), and type 1 polyketide synthase (T1PKS). As the main product, this cluster produces an asymmetric macrotriolide, which closely resembles the family of macrosphelides. The sequence of this cluster is deposited in the GenBank under the number KV441552.1. Based on this sequence, we searched for the macrosphelide biosynthesis genes in the genomes of strains VKM F-4518 and VKM F-4519 using the BLAST+ program (Table 1). The identity between the protein sequences of the genes in strain *P. sporulosa* AP3s5-JAC2a [36] and the studied *Pseudogymnoascus* strains was more than 75%. The organization of the gene cluster *Pseudogymnoascus*, as compared with that of strain *P. sporulosa*, is presented in Figure 2.

Using the antiSMASH secondary metabolite analysis tool, we scanned the genome sequences of the strains for the presence of the suspected BGC secondary metabolites. Our study showed that the genome of strain VKM F-4518 contained 32 clusters, 11 of which belonged to type 1 polyketide synthases (T1PKS), 9 to non-ribosomal peptide synthases (NRPS), 1 to type 3 polyketide synthases (T3PRS), 1 to mixed type (T1PKS, NRPS), 7 to ribosomally synthesized and post-translationally modified peptide synthases (fungal RiPP), and 3 to terpene cyclases (T) (Figure S14, Supporting Information). Strain VKM F-4519 encoded 17 clusters, 8 of which were T1PKS; 6, NRPS; 1, T3PKS, NRPS; and 2, fungal RiPP (Figure S15, Supporting Information). Strains VKM F-4518 and VKM F-4519 were found to have six BGCs, which were similar to those of the known secondary metabolites with a similarity of 12–100% (Table 2). The regions in the genomes of strains VKM F-4918–

399.1 (from 1 to 39,308) and VKM F-4919–850.1 (from 1 to 20,490)–HEx-pks1 polyketides–corresponded to the biosynthetic gene cluster of a macrotriolide from *P. sporulosa*.

Table 1. Comparison of the macrosphelide synthesis gene clusters.

***Paraphaeosphaeria sporulosa* AP3s5-JAC2a**		***Pseudogymnoascus* sp. VKM F-4518**		***Pseudogymnoascus* sp. VKM F-4519**	
Gene locus tag (protein accession)	Description	Gene locus tag (protein accession)	Protein identity with *P. sporulosa*	Gene locus tag (protein accession)	Protein identity with *P. sporulosa*
CC84DRAFT_1205319 (OAG05541.1)	DH	V500_01681 (KFY98390.1)	75.60%	V501_03182 (KFZ14540.1)	75.40%
CC84DRAFT_1216878 (OAG05542.1)	SDR	V500_01680 (KFY98389.1)	79.92%	V501_03183 (KFZ14541.1)	80.72%
CC84DRAFT_1195956 (OAG05543.1)	p450	V500_01679 (KFY98388.1)	83.91%	V501_03184 (KFZ14542.1)	83.72%
CC84DRAFT_1091541 (OAG05544.1)	SH	V500_01682 (KFY98391.1)	90.29%	V501_03181 (KFZ14539.1)	90.29%
CC84DRAFT_1091839 (OAG05545.1)	KS-AT-DH-ER-KR-ACP	V500_01683 (KFY98392.1)	85.45%	V501_03180 (KFZ14538.1)	85.28%

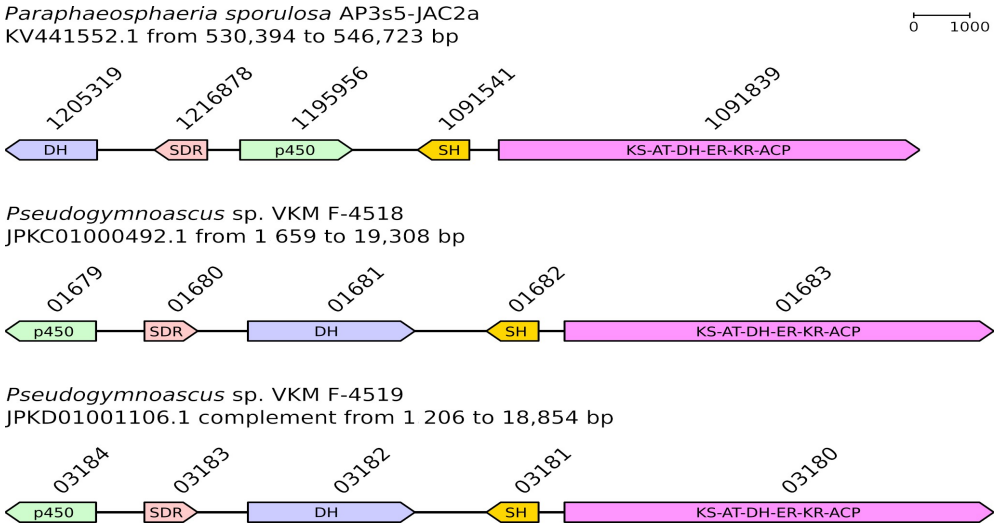

Figure 2. Organization of macrosphelide biosynthesis gene clusters.

Table 2. Clusters of the known secondary metabolites in *Pseudogymnoascus* VKM F-4518 and VKM F-4519 revealed using antiSMASH software.

Region	Type	From	To	Most Similar Known Cluster	Similarity, %
			VKM F-4518		
1.1.	T1PKS	1	15,076	Ustilaginoidins	23
53.1	T1PKS	6889	32,830	Secalonic acids	12
399.1	T1PKS	1	39,308	HEx-pks1 polyketide	100
496.1	T1PKS	4600	51,229	Orsellinic acid	50
714.1	T1PKS	1	27,887	Monacolin K	22
940.1	T1PKS	1	25,739	1,3,6,8-Tetrahydronaphthalene	100
			VKM F-4519		
183.1	T1PKS	1	43,063	Azanigerones	20
342.1	T1PKS	1	18,121	Scytalone	40
384.1	NRPS	35,666	61,986	Choline	100
850.1	T1PKS	1	20,490	HEx-pks1 polyketide	100
914.1	NRPS, T1PKS	1	32,243	Phyllostictines	20
960.1	NRPS, T1PKS	1	23,427	Phomacins D, C	22

4. Discussion

Macrosphelides A and B are metabolites of a polyketide nature belonging to 16-membered trilactone macrolides. The key structural motif of these macrolides includes a three lactone bonding, forming macrotriolides.

(+)-Macrosphelides A and B were first discovered in the fungus *Microsphaeropsis* sp. [38]. Later, 13 more natural macrosphelides were identified in *Microsphaeropsis* sp. and the fungus *Periconia byssoides*, isolated from the marine mollusk *Aplysia kurodai* [47–49]. Macrosphelides A and J were found in the fungus *Tritirachium* sp. isolated from Antarctic lichen [50]. Macrosphelide A was revealed in *Coniothyrium minitans* (current name *Paraphaeosphaeria minitans*), a mycoparasite of sclerotia-forming soil pathogens of the plants *Sclerotinia sclerotiorum*, *S. minor*, and *Sclerotium cepivorum* [51]. In the basidiomycete *Pleurotus ostreatus*, a macrosphelide was an unexpected metabolite whose biosynthesis was induced under certain conditions, namely by the addition of iodolactone, iron, copper, magnesium, and cobalt ions to the culture medium [52]. Thus, macrosphelides occur in various taxa of the fungal kingdom. For *Pseudogymnoascus* fungi, these metabolites were discovered for the first time. The studied strains are highly active producers of macrosphelides A and B in comparison to those known in the literature.

(+)-Macrosphelides A and B have antimicrobial and antitumor activity. Macrosphelide A dose-dependently inhibited the adhesion of HL-60 cells to an LPS-activated HUVEC monolayer (IC_{50}, 3.5 μM); macrophelide B also inhibited HL-60 adhesion, but to a lesser extent (IC_{50}, 36 μM) [53]. Macrosphelide A inhibited the growth of some ascomycetes, basidiomycetes, oomycetes, and Gram-positive bacteria tested, including the medically important *Staphylococcus aureus* [54]. Macrosphelide A has been shown to be capable of inhibiting the mycelial growth of *Sclerotinia sclerotiorum* and *Sclerotium sepivorum* at low concentrations (46.6 and 2.9 μg/mL, respectively) [53,55]. 3-Phenyl-macrosphelide A with higher cytotoxic properties has been obtained [56]. The apoptosis-inducing ability of hybrid compounds composed of macrosphelides and a thiazole-containing side chain of epothilones has been investigated. Among the tested series of hybrid compounds, the one containing a thiazole side chain at C15 (MSt-2) showed the maximum potency for inducing apoptosis [44,57]. The molecular mechanism of the anticancer action of macrosphelide A has been investigated [58]. This compound inhibits the proliferation of cancer cells and induces apoptosis by inhibiting the critical enzymes involved in the Warburg effect (aerobic glycolysis in cancer cells)—aldolase A, enolase 1, and fumarate hydratase. The active role of fungal macrosphelides A and B in suppressing the adhesion of human leukemia cells to the endothelial cells of the human umbilical vein, or in suppressing the growth of ovarian cancer cells, etc., makes these compounds a promising biotechnological product. Tests using monoclonal antibodies have shown that this inhibitory effect is focused on syalil Lewis, which is responsible for this adhesion [59]. At the same time, macrosphelides do not cause any significant inhibition of the growth of other cells, and thus represent a promising biotechnological product for potential drugs. Since the noteworthy biological activity of macrosphelides became apparent, attempts have been made to complete the synthesis of macrosphelides [39–46,60,61]. However, these methods of synthesis are limited by the low yield of the target products and their difficult isolation. Thus, the fungal production of macrosphelides A and B remains an object of interest.

No BGCs of macrosphelides have been described to date. Based on the comparison of the cluster of macrotriolide genes from the fungus *Paraphaeosphaeria sporulosa*, we found the complete cluster of macrosphelide biosynthesis genes in the genomes of two *Pseudogymnoascus* strains, VKM F-4518 and VKM F-4519. However, there were differences in the organization of the gene cluster. Thus, the genes for DH, SDR, and p450 were inverted in the representatives of the genus *Pseudogymnoascus*, as compared to those of strain *P. sporulosa* (Figure 2). In future, in order to experimentally prove that the BGC identified is actually responsible for the production of macrophelides, a gene knockout or heterologous expression must be performed.

Recent advances in genome sequencing have shown that there are probably over five million fungal species, with each species encoding up to 80 natural product biosynthetic pathways [36]. However, despite the increased ease of DNA sequencing, fungal cultivation remains a bottleneck, as only very limited number of fungal species are cultivated in the laboratory [62]. Even in the cultivated species, most BGCs presented in the genomes are either transcriptionally silent or expressed at an extremely low level. In our study, 32 and 17 BGCs were identified in the VKM F-4518 and VKM F-4519 strains, respectively. During our cultivation of these strains under laboratory conditions, only the biosynthetic cluster of macrosphelide genes was expressed.

5. Conclusions

(+)-Macrosphelides A and B were found in two *Pseudogymnoascus* strains, VKM F-4518 and VKM F-4519, isolated from the surface layer of sediments in the Kolyma Lowland (the Arctic). For the *Pseudogymnoascus* genus, these compounds were found for the first time. The studied strains are highly active producers of macrosphelides A, which may be a promising agent for the treatment of cancer. Based on the comparison of the cluster of macrotriolide genes from the fungus *Paraphaeosphaeria sporulosa*, we found the complete cluster of macrosphelide biosynthesis genes in the genomes of two *Pseudogymnoascus* strains, VKM F-4518 and VKM F-4519, using the BLAST+ program. On the whole, the presented study of new active arctic *Pseudogymnoascus* strains, as natural producers of macrosphelides, provides new information and a promising way of obtaining these products.

Supplementary Materials: The following supporting information can be downloaded at: https://www.mdpi.com/article/10.3390/fermentation9080702/s1, Figure S1. (a) The positive ions CI mass spectrum of 1; (b) The positive ions CI mass spectrum of 2; Table S1. Data of the NMR spectra for (+)-Macrosphelide A (1); Figure S2. ^{1}H NMR Spectrum of (+)-Macrosphelide A (1) ($CDCl_3$, RT); Figure S3. ^{13}C NMR Spectrum of (+)-Macrosphelide A (1) ($CDCl_3$, RT); Figure S4. ^{13}C APT NMR Spectrum of (+)-Macrosphelide A (1) ($CDCl_3$, RT); Figure S5. ^{1}H-^{1}H COSY NMR Spectrum of (+)-Macrosphelide A (1) ($CDCl_3$, RT); Figure S6. HSQC NMR spectrum of (+)-Macrosphelide A (1) ($CDCl_3$, RT); Figure S7. HMQC NMR Spectrum of (+)-Macrosphelide A (1) ($CDCl_3$, RT); Figure S8. HMBC NMR spectrum of (+)-Macrosphelide A (1) ($CDCl_3$, RT); Figure S9. NOESY NMR spectrum of (+)-Macrosphelide A (1) ($CDCl_3$, RT); Table S2. Data of the NMR spectra for (+)-Macrosphelide B (2); Figure S10. ^{1}H NMR Spectrum of (+)-Macrosphelide B (2) ($CDCl_3$, RT); Figure S11. ^{13}C NMR Spectrum of (+)-Macrosphelide B (2) ($CDCl_3$, RT); Figure S12. ^{13}C APT NMR Spectrum of (+)-Macrosphelide B (2) ($CDCl_3$, RT); Figure S13. HSQC NMR Spectrum of (+)-Macrosphelide B (2) ($CDCl_3$, RT); Figure S14. HMBC NMR Spectrum of (+)-Macrosphelide B (2) ($CDCl_3$, RT); Figure S15. Identified secondary metabolites regions in the genome of the strain F-4518; Figure S16. Identified secondary metabolites regions in the genome of the strain F-4519.

Author Contributions: Investigation: T.V.A., K.V.Z. and V.P.Z.; writing original draft preparation: T.V.A., K.V.Z. and S.V.T.; writing—review and editing: G.A.K. and M.B.V.; software: S.V.T.; methodology: K.V.Z. and Y.K.G., visualization: M.B.V.; funding acquisition: G.A.K. and S.V.T. All authors have read and agreed to the published version of the manuscript.

Funding: This research has received funding from the Ministry of Science and Higher Education of the Russian Federation under grant agreement No. 075-15-2021-1051. The registration of NMR spectra in this work was supported in part by M.V. Lomonosov Moscow State University Program of Development.

Institutional Review Board Statement: Not applicable.

Informed Consent Statement: Not applicable.

Data Availability Statement: Not applicable.

Acknowledgments: The authors gratefully acknowledge A.Ya. Zherebker (Skolkovo Institute of Science and Technology) for the measurements of UHRMS spectra and B.P. Baskunov (IBPM RAS) for the measurements of CI mass spectra.

Conflicts of Interest: The authors declare no conflict of interest. The funders had no role in the design of the study; in the collection, analyses, or interpretation of data; in the writing of the manuscript; or in the decision to publish the results.

References

1. Calixto, J.B. The role of natural products in modern drug discovery. *An. Acad. Bras. Cienc.* **2019**, *91*, e20190105. [CrossRef]
2. Shankar, A.; Sharma, K.K. Fungal secondary metabolites in food and pharmaceuticals in the era of multi-omics. *Appl. Microbiol. Biotechnol.* **2022**, *106*, 3465–3488. [CrossRef]
3. Keller, N.P. Fungal secondary metabolism: Regulation, function and drug discovery. *Nat. Rev. Microbiol.* **2019**, *17*, 167–180. [CrossRef]
4. Avalos, J.; Limón, M.C. Fungal Secondary Metabolism. *Encyclopedia* **2022**, *2*, 1–13. [CrossRef]
5. Conrado, R.; Gomes, T.C.; Roque, G.S.C.; De Souza, A.O. Overview of bioactive fungal secondary metabolites: Cytotoxic and antimicrobial compounds. *Antibiotics* **2022**, *11*, 1604. [CrossRef] [PubMed]
6. Antipova, T.V.; Zhelifonova, V.; Zaitsev, K.V.; Zherebker, A.; Baskunov, B.; Oprunenko, Y.F. Formation of azaphilone pigments and monasnicotinic acid by the fungus *Aspergillus cavernicola*. *J. Agric. Food Chem.* **2022**, *70*, 7122–7129. [CrossRef]
7. Antipova, T.V.; Zhelifonova, V.P.; Zaitsev, K.V.; Vainshtein, M.B. Fungal azaphilone pigments as promising natural colorants. *Microbiology* **2023**, *92*, 1–10. [CrossRef]
8. Robey, M.T.; Caesar, L.K.; Drott, M.T.; Keller, N.P.; Kelleher, N.L. An interpreted atlas of biosynthetic gene clusters from 1,000 fungal genomes. *Proc. Natl. Acad. Sci. USA* **2021**, *118*, e2020230118. [CrossRef] [PubMed]
9. Khan, A.A.; Bacha, N.; Ahmad, B.; Lutfullah, G.; Farooq, U.; Cox, R.J. Fungi as chemical industries and genetic engineering for the production of biologically active secondary metabolites. *Asian Pac. J. Trop. Biomed.* **2014**, *4*, 859–870. [CrossRef]
10. Caesar, L.K.; Butun, F.A.; Robey, M.T.; Ayon, N.J.; Gupta, R.; Dainko, D.; Bok, J.W.; Nickles, G.; Stankey, R.J.; Johnson, D.; et al. Correlative metabologenomics of 110 fungi reveals metabolite–gene cluster pairs. *Nat. Chem. Biol.* **2023**, *19*, 846–854. [CrossRef]
11. Marshall, W.A. Aerial transport of keratinaceous substrate and distribution of the fungus *Geomyces pannorum* in antarctic soils. *Microb. Ecol.* **1998**, *36*, 212–219. [CrossRef] [PubMed]
12. Ozerskaya, S.; Kochkina, G.; Ivanushkina, N.; Gilichinsky, D. Fungi in permafrost. In *Permafrost Soils. Soil Biology*; Margesin, R., Ed.; Springer: Berlin/Heidelberg, Germany, 2009; Volume 16, pp. 85–95. [CrossRef]
13. Kochkina, G.; Ivanushkina, N.; Ozerskaya, S.; Chigineva, N.; Vasilenko, O.; Firsov, S.; Spirina, E.; Gilichinsky, D. Ancient fungi in Antarctic permafrost environments. *FEMS Microbiol. Ecol.* **2012**, *82*, 501–509. [CrossRef] [PubMed]
14. Leushkin, E.V.; Logacheva, M.D.; Penin, A.A.; Sutormin, R.A.; Gerasimov, E.S.; Kochkina, G.A.; Ivanushkina, N.E.; Vasilenko, O.V.; Kondrashov, A.S.; Ozerskaya, S.M. Comparative genome analysis of *Pseudogymnoascus* spp. reveals primarily clonal evolution with small genome fragments exchanged between lineages. *BMC Genom.* **2015**, *16*, 400. [CrossRef] [PubMed]
15. Zhang, X.Y.; Zhang, Y.; Xu, X.Y.; Qi, S.H. Diverse deep-sea fungi from the south China sea and their antimicrobial activity. *Curr. Microbiol.* **2013**, *67*, 525–530. [CrossRef]
16. Kochkina, G.A.; Ivanushkina, N.E.; Akimov, V.N.; Gilichinskiĭ, D.A.; Ozerskaya, S.M. Halo- and psychrotolerant *Geomyces* fungi from arctic cryopegs and marine deposits. *Microbiology* **2007**, *76*, 31–38. [CrossRef]
17. Shcherbakova, V.A.; Kochkina, G.A.; Ivanushkina, N.E.; Laurinavichius, K.S.; Ozerskaya, S.M.; Akimenko, V.K. Growth of the fungus *Geomyces pannorum* under anaerobiosis. *Microbiology* **2010**, *79*, 845–848. [CrossRef]
18. Farrell, R.L.; Arenz, B.E.; Duncan, S.M.; Held, B.W.; Jurgens, J.A.; Blanchette, R.A. Introduced and indigenous fungi of the Ross Island historic huts and pristine areas of Antarctica. *Polar Biol.* **2011**, *34*, 1669. [CrossRef]
19. Tagawa, M.; Tamaki, H.; Manome, A.; Koyama, O.; Kamagata, Y. Isolation and characterization of antagonistic fungi against potato scab pathogens from potato field soils. *FEMS Microbiol. Lett.* **2010**, *305*, 136–142. [CrossRef]
20. Loperena, L.; Soria, V.; Varela, H.S.; Lupo, S.; Bergalli, A.; Guigou, M.; Pellegrino, A.; Bernardo, A.; Calviño, A.; Rivas, F.; et al. Extracellular enzymes produced by microorganisms isolated from maritime Antarctica. *World J. Microbiol. Biotechnol.* **2012**, *28*, 2249–2256. [CrossRef] [PubMed]
21. Poveda, G.; Gil-Durán, C.; Vaca, I.; Levicán, G.; Chávez, R. Cold-active pectinolytic activity produced by filamentous fungi associated with Antarctic marine sponges. *Biol. Res.* **2018**, *51*, 28. [CrossRef] [PubMed]
22. Furhan, J. Adaptation, production, and biotechnological potential of cold-adapted proteases from psychrophiles and psychrotrophs: Recent overview. *J. Genet. Eng. Biotechnol.* **2020**, *18*, 36. [CrossRef] [PubMed]
23. Xia, Q.; Rufty, T.; Shi, W. Predominant microbial colonizers in the root endosphere and rhizosphere of turfgrass systems: *Pseudomonas veronii*, *Janthinobacterium lividum*, and *Pseudogymnoascus* spp. *Front. Microbiol.* **2021**, *12*, 643904. [CrossRef]
24. Urbina, J.; Chestnut, T.; Allen, J.M.; Levi, T. *Pseudogymnoascus destructans* growth in wood, soil and guano substrates. *Sci. Rep.* **2011**, *11*, 763. [CrossRef] [PubMed]
25. Figueroa, L.; Jiménez, C.; Rodríguez, J.; Areche, C.; Chávez, R.; Henríquez, M.; de la Cruz, M.; Díaz, C.; Segade, Y.; Vaca, I. 3-Nitroasterric acid derivatives from an Antarctic sponge-derived *Pseudogymnoascus* sp. fungus. *J. Nat. Prod.* **2015**, *78*, 919–923. [CrossRef] [PubMed]
26. Guo, Y.Z.; Wei, Q.; Gao, J.; Liu, B.Y.; Zhang, T.; Hua, H.M.; Hu, Y.C. Metabolites of the psychrophilic fungus *Pseudogymnoascus pannorum*. *Nat. Prod. Res. Dev.* **2019**, *31*, 446–449.

27. Fujita, K.; Ikuta, M.; Nishimura, S.; Sugiyama, R.; Yoshimura, A.; Kakeya, H. Amphiol, an antifungal fungal pigment from *Pseudogymnoascus* sp. PF1464. *J. Nat. Prod.* **2021**, *84*, 986–992. [CrossRef]
28. Shi, T.; Yu, Y.Y.; Dai, J.J.; Zhang, Y.T.; Hu, W.P.; Zheng, L.; Shi, D.Y. New polyketides from the Antarctic fungus *Pseudogymnoascus* sp. HSX2#-11. *Mar. Drugs* **2021**, *19*, 168. [CrossRef]
29. Li, Y.; Sun, B.; Liu, S.; Jiang, L.; Liu, X.; Zhang, H.; Che, Y. Bioactive asterric acid derivatives from the Antarctic ascomycete fungus *Geomyces* sp. *J. Nat. Prod.* **2008**, *71*, 1643–1646. [CrossRef]
30. Parish, C.A.; de la Cruz, M.; Smith, S.K.; Zink, D.; Baxter, J.; Tucker-Samaras, S.; Collado, J.; Platas, G.; Bills, G.; Díez, M.T.; et al. Antisense-guided isolation and structure elucidation of pannomycin, a substituted cis-decalin from *Geomyces pannorum*. *J. Nat. Prod.* **2009**, *72*, 59–62. [CrossRef]
31. Purić, J.; Vieira, G.; Cavalca, L.B.; Sette, L.D.; Ferreira, H.; Vieira, M.L.C.; Sass, D.C. Activity of Antarctic fungi extracts against phytopathogenic bacteria. *Lett. Appl. Microbiol.* **2018**, *66*, 530–536. [CrossRef]
32. Vaca, I.; Chávez, R. Bioactive compounds produced by Antarctic filamentous fungi. In *Fungi of Antarctica*; Rosa, L., Ed.; Springer: Cham, Switzerland, 2019; pp. 265–283. [CrossRef]
33. Gonçalves, V.N.; Carvalho, C.R.; Johann, S.; Mendes, G.; Alves, T.M.A.; Zani, C.L.; Junior, P.A.S.; Murta, S.M.F.; Romanha, A.J.; Cantrell, C.L.; et al. Antibacterial, antifungal and antiprotozoal activities of fungal communities present in different substrates from Antarctica. *Polar Biol.* **2015**, *38*, 1143–1152. [CrossRef]
34. Shi, T.; Li, X.Q.; Zheng, L.; Zhang, Y.H.; Dai, J.J.; Shang, E.L.; Yu, Y.Y.; Zhang, Y.T.; Hu, W.P.; Shi, D.Y. Sesquiterpenoids from the Antarctic fungus *Pseudogymnoascus* sp. HSX2#-11. *Front. Microbiol.* **2021**, *12*, 688202. [CrossRef]
35. Camacho, C.; Coulouris, G.; Avagyan, V.; Ma, N.; Papadopoulos, J.; Bealer, K.; Madden, T.L. BLAST+: Architecture and applications. *BMC Bioinform.* **2009**, *10*, 421. [CrossRef]
36. Harvey, C.J.B.; Tang, M.; Schlecht, U.; Horecka, J.; Fischer, C.R.; Lin, H.C.; Li, J.; Naughton, B.; Cherry, J.; Miranda, M.; et al. HEx: A heterologous expression platform for the discovery of fungal natural products. *Sci. Adv.* **2018**, *11*, eaar5459. [CrossRef]
37. Tarlachkov, S.V.; Starodumova, I.P. TaxonDC: Calculating the similarity value of the 16S rRNA gene sequences of prokaryotes or ITS regions of fungi. *J. Bioinform. Genom.* **2017**, *3*. [CrossRef]
38. Takamatsu, S.; Kim, Y.P.; Hayashi, M.; Hiraoka, H.; Natori, M.; Komiyama, K.; Omura, S. Macrosphelide, a novel inhibitor of cell-cell adhesion molecule. II. Physiochemical properties and structural elucidation. *J. Antibiot.* **1996**, *49*, 95–98. [CrossRef]
39. Sunazuka, T.; Hirose, T.; Harigaya, Y.; Takamatsu, S.; Hayashi, M.; Komiyama, K.; Ōmura, S.; Sprengeler, P.A.; Smith, A.B. Relative and absolute stereochemistries and total synthesis of (+)-macrosphelides A and B, potent, orally bioavailable inhibitors of cell−cell adhesion. *J. Am. Chem. Soc.* **1997**, *119*, 10247–10248. [CrossRef]
40. Sunazuka, T.; Hirose, T.; Chikaraishi, N.; Harigaya, Y.; Hayashi, M.; Komiyama, K.; Sprengeler, P.A.; Smith, A.B.; Ōmura, S. Absolute stereochemistries and total synthesis of (+)/(−)-macrosphelides, potent, orally bioavailable inhibitors of cell–cell adhesion. *Tetrahedron* **2005**, *61*, 3789–3803. [CrossRef]
41. Prasad, K.R.; Gutala, P. Enantioselective total synthesis of macrosphelides A and E. *Tetrahedron* **2011**, *67*, 4514–4520. [CrossRef]
42. Kobayashi, Y.; Kumar, G.B.; Kurachi, T.; Acharya, H.P.; Yamazaki, T.; Kitazume, T. Furan ring oxidation strategy for the synthesis of macrosphelides A and B. *J. Org. Chem.* **2001**, *66*, 2011–2018. [CrossRef] [PubMed]
43. Kawaguchi, T.; Funamori, N.; Matsuya, Y.; Nemoto, H. Total synthesis of macrosphelides A, B, and E: first application of ring-closing metathesis for macrosphelide synthesis. *J. Org. Chem.* **2004**, *69*, 505–509. [CrossRef]
44. Matsuya, Y.; Kawaguchi, T.; Nemoto, H. New strategy for the total synthesis of Macrosphelides A and B based on ring-closing metathesis. *Org. Lett.* **2003**, *5*, 2939–2941. [CrossRef]
45. Paek, S.M.; Seo, S.Y.; Kim, S.H.; Jung, J.W.; Lee, Y.S.; Jung, J.K.; Suh, Y.G. Concise syntheses of (+)-macrosphelides A and B. *Org. Lett.* **2005**, *7*, 3159–3162. [CrossRef] [PubMed]
46. Paek, S.M.; Suh, Y.G. Synthetic studies on bioactive natural polyketides: Intramolecular nitrile oxide-olefin cycloaddition approach for construction of a macrolactone skeleton of macrosphelide B. *Molecules* **2011**, *16*, 4850–4860. [CrossRef]
47. Takamatsu, S.; Hiraoka, H.; Kim, Y.P.; Hayashi, M.; Natori, M.; Komiyama, K.; Omura, S. Macrosphelides C and D, novel inhibitors of cell adhesion. *J. Antibiot.* **1997**, *50*, 878–880. [CrossRef] [PubMed]
48. Yamada, T.; Minoura, K.; Tanaka, R.; Numata, A. Cell-adhesion inhibitors produced by a sea hare-derived *Periconia* sp. *J. Antibiot.* **2007**, *60*, 370–375. [CrossRef]
49. Fukami, A.; Taniguchi, Y.; Nakamura, T.; Rho, M.C.; Kawaguchi, K.; Hayashi, M.; Komiyama, K.; Omura, S. New members of the macrosphelides from *Microsphaeropsis* sp. FO-050 IV. *J. Antibiot.* **1999**, *52*, 501–504. [CrossRef] [PubMed]
50. Ivanova, V.; Kolarova, M.; Aleksieva, K.; Graefe, U.; Schlegel, B. Diphenylether and macrotriolides occurring in a fungal isolate from the antarctic lichen Neuropogon. *Prep. Biochem. Biotechnol.* **2007**, *37*, 39–45. [CrossRef]
51. McQuilken, M.P.; Gemmell, J.; Hill, R.A.; Whipps, J.M. Production of macrosphelide A by the mycoparasite *Coniothyrium minitans*. *FEMS Microbiol. Lett.* **2003**, *219*, 27–31. [CrossRef]
52. Wińska, K.; Mączka, W.; Grabarczyk, M.; Sugimoto, K.; Matsuya, Y.; Szumny, A.; Anioł, M. A macrosphelide as the unexpected product of a *Pleurotus ostreatus* strain-mediated biotransformation of halolactones containing the gem-dimethylcyclohexane ring. Part 1. *Molecules* **2016**, *21*, 859. [CrossRef]
53. Hayashi, M.; Kim, Y.P.; Hiraoka, H.; Natori, M.; Takamatsu, S.; Kawakubo, T.; Masuma, R.; Komiyama, K.; Omura, S. Macrosphelide, a novel inhibitor of cell-cell adhesion molecule. I. Taxonomy, fermentation, isolation and biological activities. *J. Antibiot.* **1995**, *48*, 1435–1439. [CrossRef] [PubMed]

54. Tomprefa, N.; McQuilken, M.P.; Hill, R.A.; Whipps, J.M. Antimicrobial activity of *Coniothyrium minitans* and its macrolide antibiotic macrosphelide A. *J. Appl. Microbiol.* **2009**, *106*, 2048–2056. [CrossRef] [PubMed]
55. Albert, D.; Dumonceaux, T.; Carisse, O.; Beaulieu, C.; Filion, C. Combining desirable traits for a good biocontrol strategy against *Sclerotinia sclerotiorum*. *Microorganisms* **2022**, *10*, 1189. [CrossRef] [PubMed]
56. Heo, Y.M.; Lee, H.; Shin, Y.K.; Paek, S.M. Development of an advanced synthetic route to macrosphelides and its application to the discovery of a more potent macrosphelide derivative. *Molecules* **2014**, *19*, 15572–15583. [CrossRef]
57. Ahmed, K.; Matsuya, Y.; Nemoto, H.; Zaidi, S.F.; Sugiyama, T.; Yoshihisa, Y.; Shimizu, T.; Kondo, T. Mechanism of apoptosis induced by a newly synthesized derivative of macrosphelides with a thiazole side chain. *Chem. Biol. Interact.* **2009**, *177*, 218–226. [CrossRef] [PubMed]
58. Song, K.; Rajasekaran, N.; Chelakkot, C.; Lee, H.S.; Paek, S.M.; Yang, H.; Jia, L.; Park, H.G.; Son, W.S.; Kim, Y.J.; et al. Macrosphelide A exhibits a specific anti-cancer effect by simultaneously inactivating ENO1, ALDOA, and FH. *Pharmaceuticals* **2021**, *14*, 1060. [CrossRef]
59. Fukami, A.; Iijima, K.; Hayashi, M.; Komiyama, K.; Omura, S. Macrosphelide B suppressed metastasis through inhibition of adhesion of sLe(x)/E -selectin molecules. *Biochem. Biophys. Res. Commun.* **2002**, *291*, 1065–1070. [CrossRef]
60. Nemoto, H.; Matsuya, Y.-J. Method for Synthesizing Macrosphelides. US Patent US 7265229B2, 9 April 2007.
61. Paek, S.M. Development of advanced macrosphelides: Potent anticancer agents. *Molecules* **2015**, *20*, 4430–4449. [CrossRef]
62. Keller, M.; Zengler, K. Tapping into microbial diversity. *Nat. Rev. Microbiol.* **2004**, *2*, 141–150. [CrossRef]

Disclaimer/Publisher's Note: The statements, opinions and data contained in all publications are solely those of the individual author(s) and contributor(s) and not of MDPI and/or the editor(s). MDPI and/or the editor(s) disclaim responsibility for any injury to people or property resulting from any ideas, methods, instructions or products referred to in the content.